Neuro-Oncology

22(6), 757–772, 2020 | doi:10.1093/neuonc/noaa030 | Advance Access date 12 February 2020

Consensus recommendations for a standardized brain tumor imaging protocol for clinical trials in brain metastases

Timothy J. Kaufmann, Marion Smits, Jerrold Boxerman, Raymond Huang, Daniel P. Barboriak, Michael Weller, Caroline Chung, Christina Tsien, Paul D. Brown, Lalitha Shankar, Evanthia Galanis, Elizabeth Gerstner, Martin J. van den Bent, Terry C. Burns, Ian F. Parney, Gavin Dunn, Priscilla K. Brastianos, Nancy U. Lin, Patrick Y. Wen, and Benjamin M. Ellingson

Department of Radiology, Mayo Clinic, Rochester, Minnesota, USA (T.J.K.); Department of Radiology and Nuclear Medicine, Erasmus Medical Center, University Medical Center Rotterdam, Rotterdam, Netherlands (M.S.); Department of Diagnostic Imaging, Rhode Island Hospital and Warren Alpert Medical School of Brown University, Providence, Rhode Island, USA (J.B.); Department of Radiology, Brigham and Women's Hospital, Boston, Massachusetts, USA (R.H.); Department of Radiology, Duke University School of Medicine, Durham, North Carolina, USA (D.P.B.); Department of Neurology & Brain Tumor Center, University Hospital and University of Zurich, Zurich, Switzerland (M.W.); Department of Radiation Oncology, The University of Texas MD Anderson Cancer Center, Houston, Texas, USA (C.C.); Department of Radiation Oncology, Johns Hopkins University, Baltimore, Maryland, USA (C.T.); Department of Radiation Oncology, Mayo Clinic, Rochester, Minnesota, USA (P.D.B.); Division of Cancer Treatment and Diagnosis, National Cancer Institute (NCI), Bethesda, Maryland, USA (L.S.); Division of Medical Oncology, Department of Oncology, Mayo Clinic, Rochester, Minnesota, USA (E.G.); Department of Neurology, Massachusetts General Hospital, Harvard Medical School, Boston, Massachusetts, USA (El.G.); Department of Neuro-Oncology, Erasmus MC Cancer Institute, Rotterdam, Netherlands (M.J.B.); Department of Neurosurgery, Mayo Clinic, Rochester, Minnesota, USA (T.C.B., I.F.P.); Department of Neurological Surgery, Washington University, St Louis, Missouri, USA (G.D.); Departments of Medicine and Neurology, Massachusetts General Hospital, Boston, Massachusetts, USA (P.K.B.); Department of Medical Oncology, Dana-Farber Cancer Institute, Harvard Medical School, Boston, Massachusetts, USA (N.U.L.); Center for Neuro-Oncology, Dana-Farber/Brigham and Women's Cancer Center, Harvard Medical School, Boston, Massachusetts, USA (P.Y.W.); UCLA Brain Tumor Imaging Laboratory, Center for Computer Vision and Imaging Biomarkers, David Geffen School of Medicine, University of California Los Angeles, Los Angeles, California, USA (B.M.E.); Departments of Radiological Sciences and Psychiatry, David Geffen School of Medicine, University of California Los Angeles, Los Angeles, California, USA (B.M.E.)

Corresponding Author: Timothy J. Kaufmann, MD, Professor of Radiology, Department of Radiology, Mayo Clinic, Rochester, MN (kaufmann.timothy@mayo.edu).

Abstract

A recent meeting was held on March 22, 2019, among the FDA, clinical scientists, pharmaceutical and biotech companies, clinical trials cooperative groups, and patient advocacy groups to discuss challenges and potential solutions for increasing development of therapeutics for central nervous system metastases. A key issue identified at this meeting was the need for consistent tumor measurement for reliable tumor response assessment, including the first step of standardized image acquisition with an MRI protocol that could be implemented in multicenter studies aimed at testing new therapeutics. This document builds upon previous consensus recommendations for a standardized brain tumor imaging protocol (BTIP) in high-grade gliomas and defines a protocol for brain metastases (BTIP-BM) that addresses unique challenges associated with assessment of CNS metastases. The "minimum standard" recommended pulse sequences include: (i) parameter matched pre- and post-contrast inversion recovery (IR)–prepared, isotropic 3D T1-weighted gradient echo (IR-GRE); (ii) axial 2D T2-weighted turbo spin echo acquired after injection of gadolinium-based contrast agent and before post-contrast 3D T1-weighted images;

(iii) axial 2D or 3D T2-weighted fluid attenuated inversion recovery; (iv) axial 2D, 3-directional diffusion-weighted images; and (v) post-contrast 2D T1-weighted spin echo images for increased lesion conspicuity. Recommended sequence parameters are provided for both 1.5T and 3T MR systems. An "ideal" protocol is also provided, which replaces IR-GRE with 3D TSE T1-weighted imaging pre- and post-gadolinium, and is best performed at 3T, for which dynamic susceptibility contrast perfusion is included. Recommended perfusion parameters are given.

Keywords

brain metastases | imaging | MRI | protocol

Need for Development of Therapeutics for Treating Brain Metastases

Brain metastases are the most common central nervous system (CNS) tumor,[1,2] with more than 150 000–200 000 new patients diagnosed with brain metastases each year in the US.[3,4] This incidence is substantially greater than that of primary malignant brain tumors.[5] The lifetime incidence of brain metastases among all cancer patients is approximately 10–30%.[2,6,7] The most common primary tumors are lung cancer, breast cancer, and melanoma, occurring in approximately 40–50%, 15–20%, and 5–20%, respectively, of newly diagnosed brain metastasis patients,[8] with melanoma having the highest predilection to metastasize to the brain (~50%).[9,10] The incidence of brain metastases appears to be increasing, in part due to an overall increase in primary cancers, as well as better systemic therapies, which increase the probability of metastatic disease as patients live longer, especially within the brain as a potential sanctuary protected by the blood–brain barrier.[2]

The discovery of brain metastases has always been very sobering, indicating disseminated malignancy and historically a dismal prognosis. However, hope is increasing at the dawn of the molecular and immunotherapeutic era, with improved local therapies such as stereotactic radiosurgery (SRS) and earlier detection of brain metastases while patients have good performance status.[11,12] Improvements in outcome for patients with brain metastases from lung cancer, breast cancer, and melanoma have all been reported, and for certain patient subsets, survival is substantially longer than historical estimates. For instance, the success of monoclonal antibodies against immune checkpoints in some cases of advanced melanoma and non-small-cell lung carcinoma (NSCLC)[13–15] gives hope for further advances with immunotherapy. Durable responses have been reported with targeted agents, including BRAF inhibitors in melanoma and other cancers, anaplastic lymphoma kinase (ALK) inhibitors in ALK+ NSCLC, and human epidermal growth factor receptor 2 (HER2) inhibitors in HER2+ breast cancer.[16–18] Other clinical trials for CNS metastases with newer targeted therapies (eg, NCT03994796) and multiple immunotherapies are currently in progress (eg, NCT02886585, NCT02939300). Use of SRS for multiple brain metastases is also rising, particularly following the results of the Alliance N0574[19] and N107C[20] trials with greater community health care penetrance of SRS. That being said, it is clear that much work still needs to be done, as prognosis following the diagnosis of brain metastasis is still often enumerated in months,[3,21,22] underscoring the need for continued development of therapeutic options for patients with brain metastases.

Need for Imaging Standardization for Improved Therapeutic Response Assessment in Brain Metastases

With new efforts at treating brain metastases in an era when the vast majority of patients are diagnosed and monitored using MR imaging, reliable methods for disease monitoring and response assessment using MR imaging data are needed. Particularly in the conduct of clinical trials, implementation of standardized brain MRI protocols is an essential first step toward achieving consistent measurement and reliable assessment of response to novel therapies, whether response is assessed using clinical response criteria or automated approaches. Such a standardized brain tumor imaging protocol (BTIP) has already been developed[23] for gliomas and is being widely adopted in glioma trials. Based on the experiences of implementing the BTIP protocol, it has become apparent that MRI protocols for clinical trials must generally also serve the function of a routine clinical MRI for standard-of-care management of patients in order to minimize duplicative imaging sessions for patients and avoid challenges with reimbursement.

A recent meeting was held on March 22, 2019, among the FDA, clinical scientists, pharmaceutical and biotech companies, clinical trials cooperative groups, and patient advocacy groups to discuss challenges and potential solutions for increasing the development of therapeutics for CNS metastases. At this meeting, the need for more consistent response assessment methodology for brain metastases was identified as a key issue, and the first step toward consistent, reliable response assessment is the standardization of image acquisition with an MRI protocol that could be implemented in the multicenter setting.

The multidisciplinary and multinational Response Assessment in Neuro-Oncology–Brain Metastases (RANO-BM) working group has developed standardized guidelines for determining response to therapy for brain metastases.[24–26] This group has provided a consensus approach to measuring brain metastases and incorporating corticosteroid dosing and clinical status into the response assessment criteria.[24] The difficult issues of response assessment following SRS and immunotherapy were also broached by this group; they stated that advanced imaging may assist in discriminating tumor progression from treatment effect in these posttreatment circumstances while acknowledging that to date, these advanced imaging techniques have not shown robust validation to justify the recommendation of any particular advanced imaging technique(s) for this purpose.[24] Finally, a supplementary appendix to the RANO-BM manuscript[24] gives a recommended minimum MRI protocol for imaging brain metastases.

However, particularly as clinical trials for brain metastases increase, and MRI technology evolves, an updated minimum recommended protocol for imaging brain metastases in clinical trials is needed. In this current effort, we use the RANO-BM appendix[24] and the similar BTIP[23] as a core of such a revised protocol, which we hope will provide meaningful and generalizable imaging data from clinical trials and which may also facilitate standard-of-care clinical evaluation and decision making.

Magnetic Resonance Imaging of Brain Metastases

The early detection of brain metastases leads to earlier interventions and has been shown to result in better quality of life.[27,28] Treatment strategies (eg, SRS vs whole brain radiation) are often based on the number and size of metastases,[29] and thus accurate imaging of brain metastases is crucial. Multiple brain metastases are common with many primary tumor histologies, though solitary metastases may be seen with some cancers.[30,31] Brain metastases are distributed proportional to blood flow, with 80% in the cerebral hemispheres, 15% in cerebellum, and 5% in the brainstem.[32,33] Brain metastases commonly occur at the interface between gray and white matter, possibly due to the change in size of arterioles from cortex to white matter.[34] However, they also occur purely within white matter as well as within cortex and deep gray matter structures.

The diagnosis of brain metastases is typically made with gadolinium-based contrast-enhanced MRI, which is superior to contrast-enhanced CT.[35–38] Prior to 2006, treatment guidelines for brain metastases were based upon studies in which metastases were diagnosed and monitored with CT.[39–41] However, the value of gadolinium-based contrast-enhanced T1-weighted imaging for the detection of brain metastases has been well documented for more than 30 years.[42–46] Almost all brain metastases enhance in their entirety, due to the lack of blood–brain and blood–tumor barriers,[34] unless the tumors have non-enhancing cystic or frankly hemorrhagic components. Brain metastases of moderate to large size are typically surrounded by substantial vasogenic edema, related to increased tumor capillary permeability and/or temporary vascular occlusion from neoplastic cell growth after hematological spread.[34] Small metastases can also present with disproportionate peritumoral edema. T2-weighted imaging and T2-weighted fluid attenuated inversion recovery (FLAIR) best detect the T2 prolongation associated with this edema in the brain. Metastases themselves vary in signal intensity on T2-weighted imaging and, while usually relatively hyperintense,[34] may be hypointense, classically associated with highly cellular neoplasms with high nuclear-to-cytoplasm ratios and with some, though not all, adenocarcinoma metastases.[34,47–49] Calcified metastases are rare but possible. Metastases vary in apparent diffusion coefficient (ADC) and appearance on diffusion-weighted imaging (DWI), and attempts have been made to correlate ADC with tumor histology and response to therapy such as SRS with limited success.[50–52]

Baseline MR Evaluation

For response assessment using the current standardized response criteria, brain metastases must be accurately measurable in at least one dimension.[24] Thin-section, preferably volumetric, T1-weighted imaging would be most desirable. Identical pre- and post-contrast T1-weighted imaging allows the subtraction of inherent T1 shortening or bright signal, which may be seen in hemorrhage (methemoglobin) from true contrast enhancement and can aid in clinical evaluation and advanced image post-processing for trials. Hemorrhage within brain metastases correlates with certain histologies (being particularly common in melanoma, renal cell carcinoma, choriocarcinoma, and thyroid carcinoma but also common in breast and lung carcinoma) and with increasing size. Overall, approximately 20% of metastases may be overtly hemorrhagic,[34,53] with two-thirds of large metastases showing evidence of hemorrhage on susceptibility weighted imaging (SWI).[54] Additionally, melanoma metastases can have T1 shortening from melanin. Therefore, a means to account for pre-contrast T1 hyperintensity in evaluating contrast enhancement is important. Pre- and post-contrast image subtraction also markedly improves contrast ratios of enhancing lesions.[55]

Improved Detection of Brain Metastases

The question of which post-contrast T1-weighted pulse sequence is "best" is complicated. The first limitations in answering this question relate to what MR scanner hardware and software a particular site possesses, including field strength (usually 1.5T vs 3T)—3T brain MRI offers signal-to-noise ratio (SNR) advantages over 1.5T, which can be traded off for better spatial resolution or decreased imaging time.[56–58] Any disadvantages of 3T are probably offset by its advantages when imaging brain metastases.[59,60] For instance, 3D fast spin echo T1-weighted techniques such as CUBE (GE Healthcare), SPACE (Sampling Perfection with Application optimized Contrasts by using different flip angle Evolutions; Siemens Healthcare), and VISTA (Volumetric Isotropic TSE Acquisition; Philips Healthcare)[61] are all improved in SNR at 3T compared with 1.5T.

Magnetization prepared ("IR-prepped") 3D gradient recalled echo (GRE) pulse sequences such as MPRAGE (magnetization-prepared rapid acquisition with gradient echo), IR-SPGR (inversion recovery–spoiled gradient),

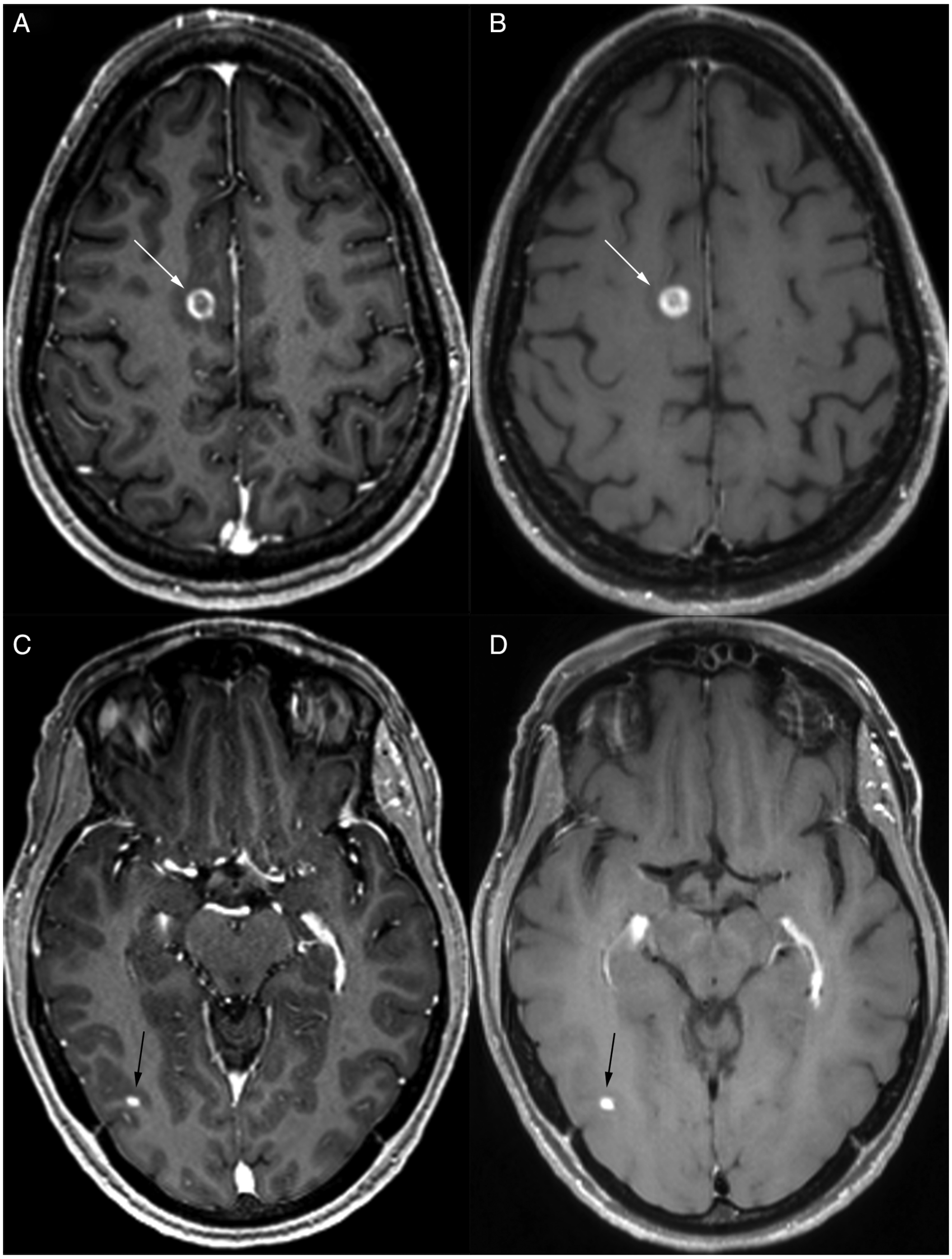

Fig. 1 Comparison of 3D IR-GRE (A, C) and 3D TSE (B, D) T1-weighted imaging in a patient with metastatic lung carcinoma to the brain. Larger lesions (eg, right posterior frontal, white arrows, A and B) are well visualized with both techniques. Smaller lesions (eg, right posterior temporal, black arrows, C and D) may be better visualized with 3D TSE T1-weighted imaging due to more native vascular signal suppression and higher contrast:noise ratio relative to underlying brain.

BRAVO (Brain Volume Imaging), TFE (turbo field echo), and 3D Fast FE (field echo) are robust, high signal-to-noise, T1-weighted pulse sequences with exquisite anatomical depiction, which are very widely available in community and academic imaging centers at both 1.5T and 3T field strengths. They form the backbone of the BTIP protocol[23] and are featured in the minimum standard protocol for brain metastases recommended in this publication. As these are 3D series, orthogonal reformats can and should be created from them, and image review should be performed in axial, sagittal, and coronal planes. However, there are disadvantages of post-contrast IR-GRE pulse sequences. The contrast enhancement of brain lesions is slightly less conspicuous with spoiled GRE-based pulse sequences than with spin echo (SE)–based pulse sequences.[62,63] The relatively bright white matter of IR-GRE yields good gray-white differentiation and depiction of anatomy, but a brightly enhancing metastasis on bright white matter then becomes less conspicuous, having a lower contrast ratio (Fig. 1). In comparison, SE-based pulse sequences including the 3D turbo SE (TSE) T1-weighted SPACE/CUBE/VISTA have relatively lower signal intensity in white matter, in part due to magnetization transfer effects,[64] increasing the contrast ratio of enhancing metastases within white matter (Fig. 1). Indeed, Knauth et al reported equivalent enhancing lesion conspicuity relative to white matter using magnetization transfer (by applying an off-resonance radiofrequency pulse to suppress background tissue signal) SE T1-weighted imaging and a single dose of gadolinium, when compared with no magnetization transfer and triple-dose gadolinium.[65] IR-GRE pulse sequences with "bright blood" contrast also make normal cortical vessels much more prominent than with SE-based pulse sequences, which have greater inherent flow suppression. (Three-dimensional TSE sequences like SPACE and CUBE have inherent flow suppression based on two mechanisms: [i] uncompensated gradient moments in the echo train which introduce intravoxel dephasing and [ii] stimulated echoes from non-180° variable flip angles which induce dephasing.) In cross section, these normal cortical vessels appear as innumerable bright dots, which can hinder the distinction of peripheral subcentimeter enhancing metastases, despite relatively high lesion SNR. Lastly, unlike with SE-based pulse sequences, it is not feasible to fat saturate IR-GRE pulse sequences, and so enhancing osseous metastases may be indistinguishable within the normally fat containing, T1-bright skull, skull base, and upper cervical vertebral marrow.

Previous studies found superior detection of brain metastasis with 3D fast spoiled gradient echo (FSPGR) or MPRAGE (with 1–1.4 mm slice thickness) compared with thick section (6–7 mm) 2D SE imaging.[63,66,67] However, a 2016 meta-analysis[68] which included 5 studies[64,69–72] comparing 3D TSE T1 (eg, SPACE) and 3D MPRAGE with equal slice thickness (1 mm) found superior detection of small metastases with 3D TSE, although these 5 studies were performed at 3T field strength only. These results are supported by other published data. Chappell et al demonstrated greater post-contrast lesion conspicuity with SE compared with GRE imaging.[73] Majigsuren et al found higher contrast-to-noise ratio (CNR) within a sampling of various brain tumors with T1-weighted CUBE (3D TSE) compared with 3D FSPGR at 3T, despite performing the post-contrast CUBE prior to the FSPGR in all instances.[74] Kammer et al reported significantly higher detectability of contrast-enhancing brain tumors with 3D TSE compared with MPRAGE at 3T with regard to number of lesions identified (particularly if small) as well as superiority of 3D TSE with regard to CNR and diagnostic confidence.[75] Danieli et al reported higher contrast rate, CNR, and visual conspicuity among metastases and gliomas with SPACE and VIBE relative to MPRAGE, and more accurate size and morphology estimates with SPACE in a 3T study.[76] Kim et al reported approximately double the detection rates of ≤5 mm brain metastases with a black blood vascular suppression (delay alternating with nutation for *tailored excitation* [DANTE]) version of SPACE compared with MPRAGE as well as higher CNR of metastases and shorter reading time with DANTE SPACE.[77] Similar to 2D TSE, 3D TSE T1-weighted images can be fat saturated, an advantage in detecting osseous metastases, unlike IR-GRE techniques like MPRAGE and BRAVO. However, 3D TSE is more challenging to acquire at 1.5T due to lower SNR. Although more recent iterations of 1.5T T1-weighted TSE seem to have acceptable SNR and lesion conspicuity, published literature for detection of brain metastases is currently still lacking. Three-dimensional TSE also may not have been a stock MRI pulse sequence with relatively older scanner purchases, and therefore, imaging centers may require an additional cost to install the sequence. It is also not standardized among MR vendors. There is not a motion-compensated version of 3D TSE, which is therefore susceptible to motion artifacts. Additionally, 3D TSE cannot be used with metallic SRS immobilization frames because eddy currents arise in the frame due to the long echo trains; GRE pulse sequences are therefore used for SRS targeting.[78]

It is also important to recognize in this discussion of ideal post-contrast T1-weighted imaging that much of the published data are concerned with the issue of metastasis detection rather than measurement. Published data on variability of measurements of brain metastases are limited.[79]

In summary, for post-contrast T1-weighted imaging, the universal availability of IR-GRE pulse sequences and their many strengths support their use in a standardized brain metastasis imaging protocol, but their limitations in identifying small metastases and osseous metastases promote the recommendation that sites also include an SE or TSE post-gadolinium T1-weighted pulse sequence, with fat suppression where possible to aid in identifying osseous metastases. The ideal choice for this pulse sequence at 3T would be 3D TSE such as CUBE, SPACE, or VISTA, which should also be fat saturated for better evaluation of osseous metastases, if available. (This sequence would effectively replace the 3D T1-weighted IR-GRE sequence.) If not available, an axial and/or coronal or 3D T1-weighted FLAIR could be considered at 3T,[55,80–82] where the inversion pulse helps null cerebrospinal fluid at 3T. At 1.5T, adding an axial and/or coronal T1-weighted SE series may increase accuracy and diagnostic confidence for small brain metastases. Disadvantages of T1-weighted SE imaging to keep in mind include ghosting artifacts due to strong signal enhancement in flowing blood, especially in the posterior fossa from the dural venous sinuses, and thicker image slices.

Other considerations for the detection of small metastases include the choice of gadolinium-based contrast agent (GBCA), its dose, and the timing of imaging following i.v. administration. High relaxivity (r1) GBCA,[83–87] double- or triple-dose GBCA,[88–97] or increased delay time, particularly with IR-GRE pulse sequences,[89,98,99] may lead to greater sensitivity for small metastases. However, some concern over gadolinium deposition in the body[100] and nephrogenic systemic fibrosis[101] has led to constraints in GBCA dosing at some local institutions, and so we provide a protocol using single-dose GBCA administration. Since delayed imaging after GBCA administration is not practical for many institutions, we do not give a uniform recommendation for an additional delay after i.v. administration of GBCA other than that introduced by performance of T2-weighted and (optional) dynamic susceptibility contrast (DSC) perfusion-weighted MRI after GBCA administration and before post-contrast T1-weighted imaging. The time interval between GBCA administration and post-contrast T1-weighted imaging can impact lesion conspicuity and apparent lesion size,[89,102] and should therefore be standardized. In our suggested protocol, the delay time will be made uniform through the inclusion of DSC-MRI and T2-weighted imaging between i.v. GBCA administration and post-contrast 3DT1-weighted imaging.

Finally, in post-processing or live image review, clinicians may also benefit from reviewing 3D post-contrast T1-weighted image sets with overlapping maximum intensity projections (eg, 10 mm sections reconstructed at 4 mm intervals), which may help with accuracy and speed of image review for small metastases.[103]

When evaluating for osseous metastases, fat-saturated T2-weighted and T2-weighted FLAIR images, at least one post-contrast T1-weighted series, and DWI are helpful. Leptomeningeal metastases may be better evaluated with post-contrast T2-weighted FLAIR than some post-contrast T1-weighted imaging,[104] which though not included in this basic protocol could be added for suspected or known leptomeningeal metastasis. Post-contrast 3D TSE T1-weighted imaging with its relative vascular signal suppression is also useful for leptomeningeal metastasis detection.[105] We also refer the reader to the RANO Leptomeningeal Response Assessment group's recommendations for leptomeningeal metastasis.[106,107]

Stereotactic Radiosurgery and Radiation Necrosis

Many brain metastases are now treated with SRS, and many if not all clinical trials for brain metastases allow for SRS. This introduces the particular challenge of response assessment for enlarging, contrast-enhancing lesions following SRS.[108,109] Approximately one-third of treated metastases will increase in size on contrast-enhanced MRI following SRS,[110] and this could represent progressive tumor and/or radiation injury, as radiation necrosis is not uncommon following SRS. This translates to roughly half of SRS-treated patients experiencing an enlarging contrast-enhancing lesion.[110] The incidence of radiation injury/necrosis depends upon the radiation dose utilized, the volume of the target lesion, and the means by which radiation necrosis is determined, but has been estimated at 6–26%.[21,111] However, it has been estimated to be as high as 60% cumulative risk for larger lesions[111] and may be higher for patients also treated with immunotherapy.[112] Radiation necrosis typically occurs 3–18 months after SRS but can occur up to 3 years post-SRS.[21] However, conventional MRI poorly differentiates between radiation necrosis and tumor or an admixture of the two,[113,114] and alternative methods using tumor segmentation[115] or delayed imaging[116] are time intensive and may be difficult to routinely employ in clinical care. Admixture of tumor and necrosis is not uncommon following SRS[109] and further complicates diagnosis.

Investigators have pursued "advanced" or physiologic/mechanistic MRI techniques, as well as other imaging modalities such as PET, to help discriminate between radiation necrosis and recurrent tumor. DWI and ADC,[117–119] MR spectroscopy,[120,121] arterial spin labeling (ASL),[122] dynamic contrast-enhanced (DCE) MRI,[119,123–125] and DSC-MRI[119,126–128] have all been evaluated in this clinical context, as have thallium-201 single-photon emission CT,[122,129] ^{18}F-FDG PET (fluorodeoxyglucose), and amino acid PET (^{11}C-methionine, ^{18}F-fluorodopa, ^{18}F-fluoro-ethyltyrosine, ^{18}F-fluorocholine).[130–138] Each of these techniques has some merit as well as unique challenges. None has been validated in multicenter trials of brain metastases treated with SRS. Some of these techniques also produce findings which may predictably evolve over time following SRS, complicating their interpretation.[139] Amino acid PET, with its low background activity in the brain, has particular promise for evaluating brain malignancies, but it is not FDA approved for brain metastases. Relatedly, it is not generally reimbursable in the United States, which makes it difficult to universally recommend. However, for trials involving other parts of the world such as Europe for which amino acid PET may be more feasible, it should certainly be considered for response assessment post-SRS.[140] Delayed contrast extravasation MRI with TRAMs (treatment response assessment maps) has also been used and shows promise,[116,141,142] including with T1 mapping and subtraction,[143] though this requires scanning at both 5 minutes and again at 60–105 minutes after i.v. GBCA administration. This may not be practical for a protocol standardized for use across many institutions and requires specific software for its analysis, but investigators could consider this if it is feasible for their sites. Future means of imaging discrimination of radiation necrosis and viable tumor could include texture analysis[144] and deep learning.[145]

DWI is included in the standardized protocols, as it was for the BTIP protocol,[23] for a few reasons. It is often included in any brain MRI, given the unique information it provides with regard to unanticipated pathology such as infarction or abscess. It can suggest tumor cellularity. It is a very fast pulse sequence, requiring only on the order of a minute of MR gradient time, and so it does not cost much to perform. Last, as DWI has been[117–119] and will likely continue to be used in clinical investigations of brain tumor response assessment, we provide it for investigators in the standardized protocols.

We encourage the use of DSC-MRI (which requires an i.v. bolus administration of GBCA) in the standardized brain metastasis imaging protocol because it may help differentiate tumor progression, characterized by higher blood volume and lower percentage signal recovery, from radiation necrosis in the post-SRS radiation treatment setting.[126–128] However, given the lack of validation of DSC-MRI for this purpose in multicenter trials, we encourage investigators to decide whether or not to mandate DSC-MRI within their own clinical trial contexts. DSC-MRI is widely available, technically robust, relatively short in acquisition time (typically on the order of 2–3 minutes), and requires no additional GBCA beyond that given for conventional post-contrast imaging. DSC-MRI requires less MRI gradient time and has substantially higher signal to noise than DCE-MRI, making it easier for a wide variety of imaging sites to perform. Based on recent computer simulations and in vivo studies, it has been suggested that DSC-MRI using a single-dose bolus of GBCA without preload, in combination with a low (eg, 30 degrees) flip-angle and post-processing leakage correction which mitigates the effect of GBCA extravasation in contrast-enhancing tumors, is an efficacious DSC-MRI protocol requiring only a single dose of GBCA.[146–148] This would be advantageous given that concerns about nephrogenic systemic fibrosis[101] and gadolinium deposition in other tissues including the brain[100] have made some centers reluctant to use supra-standard (ie, >0.1 mmol/kg) doses of gadolinium. Importantly, particularly for studies which may perform quantitative analysis of DSC-MRI, parallel imaging is advised with DSC-MRI to minimize distortion.

Interpretation of DSC-MRI for brain metastases post-SRS is beyond the scope of this effort, but suffice it to say that it should be used with caution and some skepticism in clinical practice. Indeed, published data in this setting are limited to single-institution studies; its implementation and analysis are very technique dependent,[149] and the timing of DSC relative to SRS and trends in DSC metrics over time probably matter. Generally speaking, increased blood volume and relatively low percentage signal recovery are concerning for recurrent tumor rather than radiation necrosis.[126–128] We do note that smaller lesions and peripherally located lesions near higher baseline cortical perfusion and cortical vessels are more difficult to evaluate with DSC perfusion.

Immunotherapy and Brain Metastasis Imaging

Immunotherapy has had remarkable success in different settings, including recent clinical trials demonstrating promising response rates in brain metastases from melanoma, increasing its investigation across brain metastases from many histologies. Because it purposefully stimulates a host immune reaction against tumor, it can create “pseudoprogressive” contrast enhancement due to inflammatory response rather than recurrent metastases. This creates a challenge for response assessment, which has been addressed by the RANO immunotherapy (iRANO) criteria.[150] In summary, if radiologic progression is seen within 6 months of immunotherapy, it is advised that patients remain on immunotherapy (if no clinical contraindication) for 3 months, at which time repeat imaging can be used to judge whether this represents true progressive disease.[150] Research into whether advanced imaging techniques could distinguish between pseudo- and true progression earlier in this process has only just begun.[151]

Recommended Protocol(s)

The recommended MRI protocol for use in evaluating brain metastases is highly dependent on the scanner performance and capabilities at the specific sites. A flowchart to guide decision making in terms of the recommended protocol(s) is illustrated in Fig. 2. Ideally, if sites are able to use a 3T MRI scanner and are able to perform 3D T1-weighted TSE, they should replace the 3D T1-weighted IR-GRE sequence both before and after i.v. GBCA administration (Table 1). Additionally, as a large proportion of patients receive SRS for brain metastases, we encourage but do not mandate the inclusion of DSC perfusion MRI as part of a protocol for clinical trials as it can provide complementary information to distinguish tumor progression from treatment effect in any enlarging contrast-enhancing lesion post-SRS. DSC-MRI is brief, requires no additional GBCA, and should be easily acquired at any imaging center. It will not always be helpful in distinguishing between tumor progression and radiation necrosis, but sometimes the longitudinal changes provided may. We give updated suggestions for DSC-MRI pulse sequence parameters as part of the ideal 3T protocol in Table 1. Tables 2 and 3 provide minimum standard recommended imaging parameters for

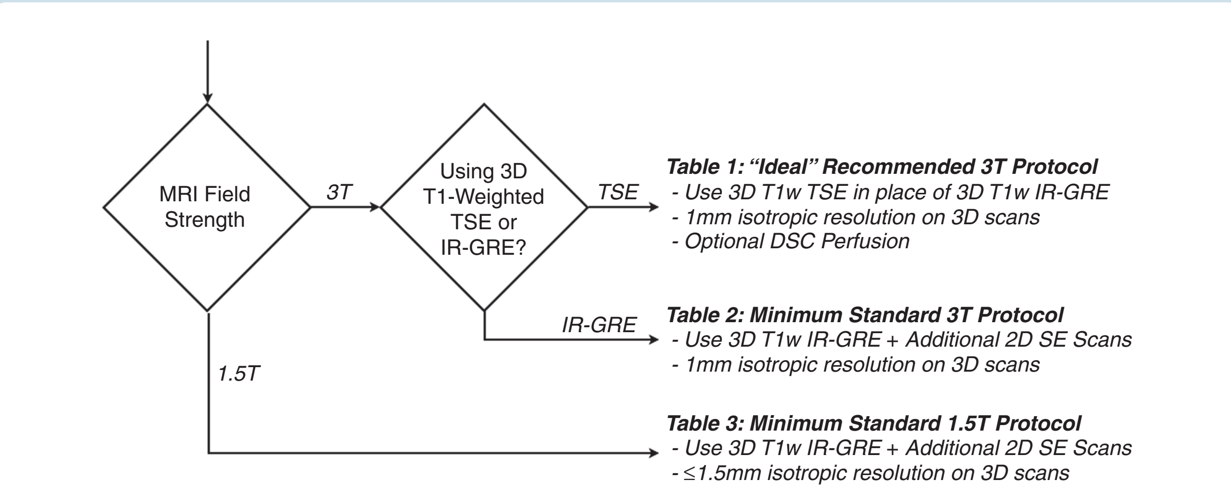

Fig. 2 Metastatic brain tumor imaging protocol decision-making flow chart. If sites are using a 3T MRI scanner and have 3D TSE available, they should use Table 1 (ideal recommended 3T protocol). If sites are using a 3T MRI scanner and *do not* have 3D TSE, they should use Table 2 (minimum standard 3T protocol). If sites use a 1.5T scanner, they should use Table 3 (minimum standard 1.5T protocol). Note that DSC perfusion may be used with the minimum standard protocols at 3T and 1.5T as well as with the “ideal” 3T protocol.

Table 1 "Ideal" recommended 3T metastatic brain tumor imaging protocol

	3D T1w TSE Pre[b]	Ax 2D FLAIR[j,q]	Ax 2D DWI[p,v]		DSC[a] Perfusion (Optional)	Ax 2D T2w[h,i,q]	3D T1w TSE Post[b]
Sequence	TSE[s]	TSE[c,s]	SS-EPI[g]	**Contrast Injection[a]**	GE-EPI	TSE[c,s]	TSE[s]
Plane	Sagittal or Axial	Axial	Axial		Axial	Axial	Sagittal or Axial
Mode	3D	2D	2D		2D	2D	3D
TR [ms]	550–750	>6000	>5000		1000–1500	>2500	550–750
TE [ms]	Min	100–140	Min		25–35 ms	80–120	Min
TI [ms]		2000–2500[k]					
Flip angle	Default[t]	90°/≥160°	90°/180°		30°	90°/≥160°	Default[t]
Frequency	256	≥256	128		≥96	≥256	256
Phase	256	≥256	128		≥96	≥256	256
NEX	≥1	≥1	≥1		1	≥1	≥1
FOV	256 mm	240 mm	240 mm		240 mm	240 mm	256 mm
Slice thickness	1 mm	3 mm	3 mm		3–5 mm as needed to cover tumor	3 mm	1 mm
Gap/spacing	0	0	0		0–1 mm as needed to cover tumor	0	0
Other options			b = 0, 500, 1000 s/mm^2 ≥3 directions		30–60 pre-bolus time points; >120 total time points		
Parallel imaging	Up to 3x[u]	Up to 2x	Up to 2x		Up to 2x	Up to 2x	Up to 3x[u]

Abbreviations: TR = repetition time; TE = echo time; TI = inversion time; NEX = number of excitations; FOV = field of view.
[a] 0.1 mmol/kg dose injection with a gadolinium chelated contrast agent. Use of a power injector is desirable at an injection rate of 3–5 cc/sec. (Note: If DSC perfusion is collected, contrast injection is performed after starting DSC acquisition. DSC perfusion can be performed with the "ideal" protocol at 3T as well as with the minimum standard protocols at 3T and 1.5T.)
[b] Post-contrast 3D T1-weighted images should be collected with equivalent parameters to pre-contrast 3D T1-weighted images.
[c] TSE = turbo spin echo (Siemens & Philips) is equivalent to FSE (fast spin echo; GE, Hitachi, Toshiba).
[d] FL2D = two-dimensional fast low angle shot (FLASH; Siemens) is equivalent to the spoil gradient recalled echo (SPGR; GE) or T1- fast field echo (FFE; Philips), fast field echo (FastFE; Toshiba), or the radiofrequency spoiled steady state acquisition rewound gradient echo (RSSG; Hitachi). A fast gradient echo sequence without inversion preparation is desired.
[e] IR-GRE = inversion-recovery gradient-recalled echo sequence is equivalent to MPRAGE = magnetization prepared rapid gradient-echo (Siemens & Hitachi) and the inversion recovery spoiled gradient-echo (IR-SPGR or Fast SPGR with inversion activated or BRAVO; GE), 3D turbo field echo (TFE; Philips), or 3D fast field echo (3D Fast FE; Toshiba).
[f] A 3D acquisition without inversion preparation will result in different contrast compared with MPRAGE or another IR-prepped 3D T1-weighted sequences and therefore should be avoided.
[g] In the event of significant patient motion, a radial acquisition scheme may be used (eg, BLADE [Siemens], PROPELLER [GE], MultiVane [Philips], RADAR [Hitachi], or JET [Toshiba]); however, this acquisition scheme is can cause significant differences in ADC quantification and therefore should be used only if EPI is not an option. Further, this type of acquisition takes considerable more time.
[h] Dual echo PD/T2 TSE is optional for possible quantification of tissue T2. For this sequence, PD is recommended to have a TE < 25ms.
[i] Advanced sequences can be substituted into this time slot, so long as 3D post-contrast T1-weighted images are collected between 4 and 8 min after contrast injection and this timing is constant across all MR exams performed in each patient.
[j] 3D FLAIR is an optional alternative to 2D FLAIR, with sequence parameters as follows per EORTC guidelines: 3D TSE/FSE acquisition; TE = 90–140 ms; TR = 6000–10,000 ms; TI = 2000–2500 ms (chosen based on vendor recommendations for optimized protocol and field strength); GRAPPA≤2; Fat Suppression; Slice thickness ≤ 1.5mm; Orientation Sagittal or Axial; FOV ≤ 250 mm x 250 mm; Matrix ≥ 244x244.
[k] Choice of TI should be chosen based on the magnetic field strength of the system (eg, TI ≈ 2000ms for 1.5T and TI ≈ 2500ms for 3T).
[l] In order to ensure comparable SNR older 1.5T MR systems can use contiguous (no interslice gap) images with 5mm slice thickness or increase NEX for slice thickness ≤4mm.
[m] For Siemens and Hitachi scanners. GE, Philips, and Toshiba scanners should use a TR = 5–15 ms for similar contrast.
[n] For Siemens and Hitachi scanners. GE, Philips, and Toshiba scanners should use a TI = 400–450 ms for similar contrast.
[p] Older model MR scanners that are not capable of >2 b-values should use b = 0 and 1000 s/mm^2.
[q] Axial 2D T2-weighted FLAIR and Axial 2D T2-weighted images can be interchanged pre- and post-contrast.
[r] Sites may choose to perform the 3D T1w IR-GRE sequence prior to the 2D T1w TSE/SE because of the potential risk of patient movement and to help with patient comfort. However, there is less inherent lesion conspicuity in the 3D T1w IR-GRE sequence, so delaying this sequence to the end may be efficacious.
[s] Acceptable 3D T1w TSE sequences include CUBE (GE), SPACE (Siemens), VISTA (Philips), isoFSE (Hitachi), or 3D MVOX (Canon)
[t] Flip angles for 3D TSE sequences (including CUBE and SPACE) are complicated because many utilize variable flip angle refocusing radiofrequency pulses to produce the desired image contrast. Investigators are encouraged to work with their scanner vendors to determine the ideal parameters.
[u] Investigators are encouraged to work with their scanner vendors to determine the best parallel imaging strategies, which may include simultaneous multislice imaging (SMS), controlled aliasing in parallel imaging resulting in higher acceleration (CAIPI), iPAT, GRAPPA, as well as turbo or other acceleration factors.
[v] While some sites may choose to collect DWI post-contrast, studies have suggested this can lower ADC measurements as much as 3%.[152]

Table 2 Minimum standard 3T metastatic brain tumor imaging protocol

	3D T1w Pre[b]	Ax 2D FLAIR[j,q]	Ax 2D DWI[p,u]		Ax 2D T2w[h,i,q]	2D SE T1w Post[r,s]	3D T1w Post[b,r]
Sequence	IR-GRE[d,e,f]	TSE[c]	SS-EPI[g]	**Contrast Injection** [a]	TSE[c]	TSE/SE	IR-GRE [d,e,f]
Plane	Sagittal or Axial	Axial	Axial		Axial	Axial and/or Coronal	Sagittal or Axial
Mode	3D	2D	2D		2D	2D	3D
TR [ms]	2100[m]	>6000	>5000		>2500	< 500	2100[m]
TE [ms]	Min	100–140	Min		80–120	Min	Min
TI [ms]	1100[n]	2000–2500[k]					1100[n]
Flip angle	10°-15°	90°/≥160°	90°/180°		90°/≥160°	90°/≥160°	10°-15°
Frequency	256	≥256	128		≥256	≥256	256
Phase	256	≥256	128		≥256	≥256	256
NEX	≥1	≥1	≥1		≥1	≥1	≥1
FOV	256 mm	240 mm	240 mm		240 mm	240 mm	256 mm
Slice thickness	1 mm	3 mm	3 mm		3 mm	3 mm	1 mm
Gap/spacing	0	0	0		0	0	0
Other options			*b* = 0, 500, 1000 s/mm^2 ≥3 directions			Fat suppression encouraged	
Parallel imaging	Up to 3x [t]	Up to 2x	Up to 2x		Up to 2x	Up to 2x	Up to 3x [t]

Abbreviations: TR = repetition time; TE = echo time; TI = inversion time; NEX = number of excitations; FOV = field of view.
[a] 0.1 mmol/kg dose injection with a gadolinium chelated contrast agent. Use of a power injector is desirable at an injection rate of 3–5 cc/sec. (Note: If DSC perfusion is collected, contrast injection is performed after starting DSC acquisition. DSC perfusion can be performed with the "ideal" protocol at 3T as well as with the minimum standard protocols at 3T and 1.5T.)
[b] Post-contrast 3D T1-weighted images should be collected with equivalent parameters to pre-contrast 3D T1-weighted images.
[c] TSE = turbo spin echo (Siemens & Philips) is equivalent to FSE (fast spin echo; GE, Hitachi, Toshiba).
[d] FL2D = two-dimensional fast low angle shot (FLASH; Siemens) is equivalent to the spoil gradient recalled echo (SPGR; GE) or T1- fast field echo (FFE; Philips), fast field echo (FastFE; Toshiba), or the radiofrequency spoiled steady state acquisition rewound gradient echo (RSSG; Hitachi). A fast gradient echo sequence without inversion preparation is desired.
[e] IR-GRE = inversion-recovery gradient-recalled echo sequence is equivalent to MPRAGE = magnetization prepared rapid gradient-echo (Siemens & Hitachi) and the inversion recovery spoiled gradient-echo (IR-SPGR or Fast SPGR with inversion activated or BRAVO; GE), 3D turbo field echo (TFE; Philips), or 3D fast field echo (3D Fast FE; Toshiba).
[f] A 3D acquisition without inversion preparation will result in different contrast compared with MPRAGE or another IR-prepped 3D T1-weighted sequences and therefore should be avoided.
[g] In the event of significant patient motion, a radial acquisition scheme may be used (eg, BLADE [Siemens], PROPELLER [GE], MultiVane [Philips], RADAR [Hitachi], or JET [Toshiba]); however, this acquisition scheme is can cause significant differences in ADC quantification and therefore should be used only if EPI is not an option. Further, this type of acquisition takes considerable more time.
[h] Dual echo PD/T2 TSE is optional for possible quantification of tissue T2. For this sequence, PD is recommended to have a TE < 25ms.
[i] Advanced sequences can be substituted into this time slot, so long as 3D post-contrast T1-weighted images are collected between 4 and 8 min after contrast injection.
[j] 3D FLAIR is an optional alternative to 2D FLAIR, with sequence parameters as follows per EORTC guidelines: 3D TSE/FSE acquisition; TE = 90–140 ms; TR = 6000–10,000 ms; TI = 2000–2500 ms (chosen based on vendor recommendations for optimized protocol and field strength); GRAPPA≤2; Fat Suppression; Slice thickness ≤ 1.5mm; Orientation Sagittal or Axial; FOV ≤ 250 mm x 250 mm; Matrix ≥ 244x244.
[k] Choice of TI should be chosen based on the magnetic field strength of the system (eg, TI ≈ 2000ms for 1.5T and TI ≈ 2500ms for 3T).
[l] In order to ensure comparable SNR older 1.5T MR systems can use contiguous (no interslice gap) images with 5mm slice thickness or increase NEX for slice thickness ≤4mm.
[m] For Siemens and Hitachi scanners. GE, Philips, and Toshiba scanners should use a TR = 5–15 ms for similar contrast.
[n] For Siemens and Hitachi scanners. GE, Philips, and Toshiba scanners should use a TI = 400–450 ms for similar contrast.
[p] Older model MR scanners that are not capable of >2 *b*-values should use *b* = 0 and 1000 s/mm^2.
[q] Axial 2D T2-weighted FLAIR and Axial 2D T2-weighted images can be interchanged pre- and post-contrast.
[r] Sites may choose to perform the 3D T1w IR-GRE sequence prior to the 2D T1w TSE/SE because of the potential risk of patient movement and to help with patient comfort. However, there is less inherent lesion conspicuity in the 3D T1w IR-GRE sequence, so delaying this sequence to the end may be efficacious.
[s] Adding FLAIR to this T1-weighted imaging at 3T could be considered for CSF suppression.
[t] Investigators are encouraged to work with their scanner vendors to determine the best parallel imaging strategies, which may include simultaneous multislice imaging (SMS), controlled aliasing in parallel imaging resulting in higher acceleration (CAIPI), iPAT, GRAPPA, as well as turbo or other acceleration factors.
[u] While some sites may choose to collect DWI post-contrast, studies have suggested this can lower ADC measurements as much as 3%.[152]

Table 3 Minimum standard 1.5T metastatic brain tumor imaging protocol

	3D T1w Pre[b]	Ax 2D FLAIR[j,q]	Ax 2D DWI[p,t]		Ax 2D T2w[h,i,q]	2D SE T1w Post[r]	3D T1w Post[b,r]
Sequence	IR-GRE [d,e,f]	TSE[c]	SS-EPI[g]	**Contrast Injection [a]**	TSE[c]	TSE/SE	IR-GRE [d,e,f]
Plane	Sagittal or Axial	Axial	Axial		Axial	Axial and/or Coronal	Sagittal or Axial
Mode	3D	2D	2D		2D	2D	3D
TR [ms]	2100[m]	>6000	>5000		>3500	400–600	2100[m]
TE [ms]	Min	100–140	Min		80–120	Min	Min
TI [ms]	1100[n]	2000–2500[k]					1100[n]
Flip angle	10°-15°	90°/≥160°	90°/180°		90°/≥160°	90°/≥160°	10°-15°
Frequency	≥172	≥256	128		≥256	≥256	≥172
Phase	≥172	≥256	128		≥256	≥256	≥172
NEX	≥1	≥1	≥1		≥1	≥1	≥1
FOV	256 mm	240 mm	240 mm		240 mm	240 mm	256 mm
Slice thickness	≤1.5 mm	≤4 mm[l]	≤4 mm[l]		≤4 mm[l]	≤4 mm[l]	≤1.5 mm
Gap/spacing	0	0	0		0	0	0
Other options			*b* = 0, 500, 1000 s/mm^2 ≥3 directions			Fat suppression encouraged	
Parallel Imaging	Up to 2x[s]	Up to 2x	Up to 2x		Up to 2x	Up to 2x	Up to 2x[s]

Abbreviations: TR = repetition time; TE = echo time; TI = inversion time; NEX = number of excitations; FOV = field of view.
[a] 0.1 mmol/kg dose injection with a gadolinium chelated contrast agent. Use of a power injector is desirable at an injection rate of 3–5 cc/sec. (Note: If DSC perfusion is collected, contrast injection is performed after starting DSC acquisition)
[b] Post-contrast 3D T1-weighted images should be collected with equivalent parameters to pre-contrast 3D T1-weighted images
[c] TSE = turbo spin echo (Siemens & Philips) is equivalent to FSE (fast spin echo; GE, Hitachi, Toshiba)
[d] FL2D = two-dimensional fast low angle shot (FLASH; Siemens) is equivalent to the spoil gradient recalled echo (SPGR; GE) or T1- fast field echo (FFE; Philips), fast field echo (FastFE; Toshiba), or the radiofrequency spoiled steady state acquisition rewound gradient echo (RSSG; Hitachi). A fast gradient echo sequence without inversion preparation is desired.
[e] IR-GRE = inversion-recovery gradient-recalled echo sequence is equivalent to MPRAGE = magnetization prepared rapid gradient-echo (Siemens & Hitachi) and the inversion recovery spoiled gradient-echo (IR-SPGR or Fast SPGR with inversion activated or BRAVO; GE), 3D turbo field echo (TFE; Philips), or 3D fast field echo (3D Fast FE; Toshiba).
[f] A 3D acquisition without inversion preparation will result in different contrast compared with MPRAGE or another IR-prepped 3D T1-weighted sequences and therefore should be avoided.
[g] In the event of significant patient motion, a radial acquisition scheme may be used (eg, BLADE [Siemens], PROPELLER [GE], MultiVane [Philips], RADAR [Hitachi], or JET [Toshiba]); however, this acquisition scheme is can cause significant differences in ADC quantification and therefore should be used only if EPI is not an option. Further, this type of acquisition takes considerable more time.
[h] Dual echo PD/T2 TSE is optional for possible quantification of tissue T2. For this sequence, PD is recommended to have a TE < 25ms.
[i] Advanced sequences can be substituted into this time slot, so long as 3D post-contrast T1-weighted images are collected between 4 and 8 min after contrast injection.
[j] 3D FLAIR is an optional alternative to 2D FLAIR, with sequence parameters as follows per EORTC guidelines: 3D TSE/FSE acquisition; TE = 90–140 ms; TR = 6000–10,000 ms; TI = 2000–2500 ms (chosen based on vendor recommendations for optimized protocol and field strength); GRAPPA≤2; Fat Suppression; Slice thickness ≤ 1.5mm; Orientation Sagittal or Axial; FOV ≤ 250 mm x 250 mm; Matrix ≥ 244x244.
[k] Choice of TI should be chosen based on the magnetic field strength of the system (eg, TI ≈ 2000ms for 1.5T and TI ≈ 2500ms for 3T).
[l] In order to ensure comparable SNR older 1.5T MR systems can use contiguous (no interslice gap) images with 5mm slice thickness or increase NEX for slice thickness ≤4mm.
[m] For Siemens and Hitachi scanners. GE, Philips, and Toshiba scanners should use a TR = 5–15 ms for similar contrast.
[n] For Siemens and Hitachi scanners. GE, Philips, and Toshiba scanners should use a TI = 400–450 ms for similar contrast.
[p] Older model MR scanners that are not capable of >2 *b*-values should use *b* = 0 and 1000 s/mm^2.
[q] Axial 2D T2-weighted FLAIR and Axial 2D T2-weighted images can be interchanged pre- and post-contrast.
[r] Sites may choose to perform the 3D T1w IR-GRE sequence prior to the 2D T1w TSE/SE because of the potential risk of patient movement and to help with patient comfort. However, there is less inherent lesion conspicuity in the 3D T1w IR-GRE sequence, so delaying this sequence to the end may be efficacious.
[s] Investigators are encouraged to work with their scanner vendors to determine the best parallel imaging strategies, which may include simultaneous multislice imaging (SMS), controlled aliasing in parallel imaging resulting in higher acceleration (CAIPI), iPAT, GRAPPA, as well as turbo or other acceleration factors.
[t] While some sites may choose to collect DWI post-contrast, studies have suggested this can lower ADC measurements as much as 3%.[152]

evaluation of brain metastases at 3T and 1.5T, respectively. These minimum protocols include imaging series that will be familiar to current users of the BTIP.

The standard protocol limits GBCA administration to a single-dose (0.1 mmol/kg) bolus, based on recent data on DSC-MRI accuracy in the primary brain tumor setting,[146,147] but we also allow for double, 0.2 mmol/kg total GBCA dosing if investigators and sites prefer. If a double dose of GBCA is used and DSC perfusion is performed, the first GBCA dose should be used as gadolinium preload, preceding the DSC series, which would then use the second GBCA dose. A higher relaxivity GBCA, for greater lesion contrast conspicuity and possibly improved DSC signal change (especially at 1.5T), is preferable but not mandated.

If sites have 3T scanners and if patients have no contraindications to scanning at 3T, we recommend acquiring brain imaging at 3T over 1.5T, as the advantages at 3T outweigh disadvantages. The current literature suggests that the most sensitive pulse sequence for the detection of small metastases is 3D TSE T1-weighted imaging with greater sensitivity at 3T compared with 1.5T. Three-dimensional TSE T1-weighted imaging at 1.5T has not been well evaluated for brain metastasis detection, and its quality can vary depending upon scanner platform. Therefore, we recommend 3D TSE T1-weighted imaging be used at 3T but cannot universally endorse it at 1.5T until additional studies are conducted.

For sites not able to perform stand-alone 3D TSE T1-weighted imaging and would use the "standard" protocol with 3D IR-GRE instead, we recommend the addition of one post-contrast 2D SE or TSE T1-weighted series at the conclusion of the MR exam both for clinical purposes and for trial outcome purposes. This can assist in the detection of small metastases that may not be detected on IR-GRE imaging or which may be obscured by artifacts that differ between the 2 post-contrast pulse sequences. For instance, a second post-contrast T1-weighted series may increase diagnostic confidence when considering SRS to new very small metastases, or if artifacts are present in a particular location on one imaging series. Although we advocate for acquisition of this additional sequence, we are not providing specific parameters for the second post-contrast T1-weighted series because: (i) we encourage sites to perform their best possible pulse sequence, which may vary significantly, and (ii) for clinical trial evaluation purposes and generalizability, the 3D post-contrast T1-weighted scan should be used for measurements and advanced image post-processing, whereas the post-contrast SE or TSE series can be used in a qualitative way to support the accuracy of the BTIP-based protocol. We recommend that such a 2D SE/TSE T1-weighted series have slice thickness no greater than 4 mm and no interslice gap.

Acknowledging that some imaging sites may routinely perform *either* turbo spin echo T2-weighted *or* T2-weighted FLAIR imaging in order to reduce exam time, we recommend acquiring both. Current automated segmentation algorithms utilize both T2- and T2-weighted FLAIR, which may be important for some trials. However, if sites are able to acquire only one of these sequences, primary investigators could consider this as acceptable, although less optimal. For instance, primarily cystic metastases may be best appreciated on T2-weighted imaging.

As T2-weighted FLAIR is also performed pre-GBCA administration at some sites, and post-GBCA administration at others, we also allow for investigators and/or sites to choose this timing of T2-weighted FLAIR, simply pointing out that post-contrast T2-weighted FLAIR will depict as bright not only lesions with T2 lengthening but also GBCA-enhancing lesions. Advantages of performing T2-weighted FLAIR post-gadolinium include the potentially better conspicuity of leptomeningeal metastases and some parenchymal metastases. Lastly, it is crucial that at least one pulse sequence be performed between the administration of GBCA and the first post-contrast T1-weighted series, to optimize lesion contrast enhancement. Typically, T2-weighted imaging is performed as this temporal "spacer," since GBCA enhancement is not detectable in non-FLAIR T2-weighted images. However, if sites do not perform routine T2-weighted imaging, they will need another pulse sequence such as a T2-weighted FLAIR at this time point in the imaging protocol.

Some imaging centers routinely perform susceptibility weighted imaging (SWI), which has very good sensitivity for paramagnetic substances such as hemosiderin in hemorrhagic tumors and deoxyhemoglobin in veins. SWI indicates the presence of hemorrhage in many metastases,[54] which may have some utility in their evaluation, though SWI alone is not as sensitive for small metastases as is post-contrast T1-weighted imaging. Investigators should feel free to include SWI or allow it if desired; its only downside is that it requires MR gradient time on the order of 5 minutes.

It is strongly encouraged that imaging centers employ the same MRI scanner platform, including field strength, and the same imaging protocol, at all scan time points for any given patient. This will aid in accurately evaluating imaging changes over time. A cautionary note for clinical investigators is warranted here. The clear advantages to the "ideal" protocol over the "minimum standard" protocol justify its being used whenever possible, and its inclusion in this document could serve to also better inform sites when they are upgrading their MRI equipment. However, because many sites will not be able to perform the "ideal" protocol or may have only a single or limited number of capable scanners, this could present a challenge to performing follow-up MR exams on a given patient on the same scanner platform. This underscores the need for clear communication and cooperation with radiology departments or imaging centers.

The aforementioned protocol is meant to provide a fundamental standard for use in clinical trials involving brain metastases. Sites are welcome to add additional pulse sequences to meet their particular clinical needs. For example, some sites may feel more comfortable always acquiring a second, confirmatory post-contrast T1-weighted sequence for greater certainty in identifying small metastases, particularly if there are artifacts. Also, sites may consider adding other imaging techniques with which they have experience and skill, such as 1-hour delayed post-contrast T1-weighted imaging, ASL, DCE, MR spectroscopy, or PET for better differentiation of radiation necrosis and recurrent tumor in the post-SRS setting.

Conclusion

Brain metastases present some unique imaging challenges compared with gliomas. We therefore provide suggestions for a “minimum standard” as well as “ideal” MR imaging protocols, depending on imaging sites’ capabilities, that should serve well for clinical purposes as well as for patients with brain metastases on clinical trials.

Funding

None.

Conflict of interest statement: Patrick Wen: research support: Agios, Astra Zeneca/Medimmune, Beigene, Celgene, Eli Lily, Genentech/Roche, Kazia, MediciNova, Merck, Novartis, Oncoceutics, Vascular Biogenics, VBI Vaccines. Priscilla Brastianos: research funding: Merck, BMS, Lilly, Pfizer. Raymond Huang: research support: Agios Pharmaceuticals (not relevant to topic). Michael Weller: research grants from Abbvie, Adastra, Bristol-Myers Squibb (BMS), Dracen, Merck, Sharp & Dohme (MSD), Merck (EMD), Novocure, Piqur, and Roche. Eva Galanis: research funding: MedImmune, Inc, Denovo Biopharma, Tracon, Genentech, Bristol-Myers Squibb. Caroline Chung: research funding: Siemens. Nancy Lin: research funding: Merck, Pfizer, Genentech, Seattle Genetics.

Advisory affiliations. Patrick Wen: Agios, Astra Zeneca, Bayer, Blue Earth Diagnostics, Immunomic Therapeutics, Karyopharm, Kiyatec, Puma, Taiho, Vascular Biogenics, Deciphera, VBI Vaccines, Tocagen, Voyager. Priscilla Brastianos: Tesaro, Angiochem, Lilly, Genentech-Roche. Dan Barboriak: Blue Earth Diagnostics; GE Neuro MRI (no reimbursement). Terry Burns: Neurametrix.

Management affiliations: Marion Smits: On national guideline committee for Brain Metastasis in the Netherlands.

Paid consulting: Patrick Wen: Merck, Prime Oncology. Priscilla Brastianos: Genentech-Roche, Merck, ElevateBio. Eva Galanis: General Consulting: MedImmune, Inc; F. Hoffman La Roche, Ltd (compensation to Mayo) Tactical Therapeutics, Inc; Oncorus (personal compensation); and Advisory Board: Vyriad (compensation to Mayo). Celgene Corporation; KIYATEC (personal compensation). Paul Brown: UpToDate contributor (personal compensation). Marion Smits: GE Healthcare (speaker fees). Michael Weller: Honoraria for lectures or advisory board participation or consulting from Abbvie, Basilea, Bristol-Myers Squibb (BMS), Celgene, Merck, Sharp & Dohme (MSD), Merck (EMD), Novocure, Orbus, Roche, and Tocagen. Nancy Lin: Consulting/advisory board: Seattle Genetics, Daiichi Sankyo.

References

1. Tabouret E, Chinot O, Metellus P, Tallet A, Viens P, Gonçalves A. Recent trends in epidemiology of brain metastases: an overview. *Anticancer Res*. 2012;32(11):4655–4662.
2. Wen PY, Black PM, Loeffler JS. Metastatic brain cancer. In: DeVita V, Hellman S, Rosenberg SA, eds. *Cancer: Principles and Practice of Oncology*. 6th ed. Philadelphia, PA: Lippincott, Williams, & Wilkins; 2001:2655–2670.
3. Stelzer KJ. Epidemiology and prognosis of brain metastases. *Surg Neurol Int*. 2013;4(Suppl 4):S192–S202.
4. Arvold ND, Lee EQ, Mehta MP, et al. Updates in the management of brain metastases. *Neuro Oncol*. 2016;18(8):1043–1065.
5. Davis FG, Dolecek TA, McCarthy BJ, Villano JL. Toward determining the lifetime occurrence of metastatic brain tumors estimated from 2007 United States cancer incidence data. *Neuro Oncol*. 2012;14(9):1171–1177.
6. Nayak L, Lee EQ, Wen PY. Epidemiology of brain metastases. *Curr Oncol Rep*. 2012;14(1):48–54.
7. Barnholtz-Sloan JS, Sloan AE, Davis FG, Vigneau FD, Lai P, Sawaya RE. Incidence proportions of brain metastases in patients diagnosed (1973 to 2001) in the Metropolitan Detroit Cancer Surveillance System. *J Clin Oncol*. 2004;22(14):2865–2872.
8. Eichler AF, Plotkin SR. Brain metastases. *Curr Treat Options Neurol*. 2008;10(4):308–314.
9. Amer MH, Al-Sarraf M, Baker LH, Vaitkevicius VK. Malignant melanoma and central nervous system metastases: incidence, diagnosis, treatment and survival. *Cancer*. 1978;42(2):660–668.
10. O'Neill BP, Buckner JC, Coffey RJ, Dinapoli RP, Shaw EG. Brain metastatic lesions. *Mayo Clin Proc*. 1994;69(11):1062–1068.
11. Sperduto PW, Kased N, Roberge D, et al. Summary report on the graded prognostic assessment: an accurate and facile diagnosis-specific tool to estimate survival for patients with brain metastases. *J Clin Oncol*. 2012;30(4):419–425.
12. Sperduto PW, Yang TJ, Beal K, et al. Estimating survival in patients with lung cancer and brain metastases: an update of the graded prognostic assessment for lung cancer using molecular markers (Lung-molGPA). *JAMA Oncol*. 2017;3(6):827–831.
13. Franklin C, Livingstone E, Roesch A, Schilling B, Schadendorf D. Immunotherapy in melanoma: recent advances and future directions. *Eur J Surg Oncol*. 2017;43(3):604–611.
14. Tawbi HA, Forsyth PA, Algazi A, et al. Combined nivolumab and ipilimumab in melanoma metastatic to the brain. *N Engl J Med*. 2018;379(8):722–730.
15. Long GV, Atkinson V, Lo S, et al. Combination nivolumab and ipilimumab or nivolumab alone in melanoma brain metastases: a multicentre randomised phase 2 study. *Lancet Oncol*. 2018;19(5):672–681.
16. Gadgeel S, Peters S, Mok T, et al. Alectinib versus crizotinib in treatment-naive anaplastic lymphoma kinase-positive (ALK+) non-small-cell lung cancer: CNS efficacy results from the ALEX study. *Ann Oncol*. 2018;29(11):2214–2222.
17. Solomon BJ, Besse B, Bauer TM, et al. Lorlatinib in patients with ALK-positive non-small-cell lung cancer: results from a global phase 2 study. *Lancet Oncol*. 2018;19(12):1654–1667.
18. Freedman RA, Gelman RS, Anders CK, et al; Translational Breast Cancer Research Consortium. TBCRC 022: a phase II trial of neratinib and capecitabine for patients with human epidermal growth factor receptor 2-positive breast cancer and brain metastases. *J Clin Oncol*. 2019;37(13):1081–1089.
19. Brown PD, Jaeckle K, Ballman KV, et al. Effect of radiosurgery alone vs radiosurgery with whole brain radiation therapy on cognitive function in patients with 1 to 3 brain metastases: a randomized clinical trial. *JAMA*. 2016;316(4):401–409.
20. Brown PD, Ballman KV, Cerhan JH, et al. Postoperative stereotactic radiosurgery compared with whole brain radiotherapy for resected metastatic brain disease (NCCTG N107C/CEC·3): a multicentre, randomised, controlled, phase 3 trial. *Lancet Oncol*. 2017;18(8):1049–1060.

21. Sneed PK, Mendez J, Vemer-van den Hoek JG, et al. Adverse radiation effect after stereotactic radiosurgery for brain metastases: incidence, time course, and risk factors. *J Neurosurg.* 2015;123(2):373–386.
22. Sahgal A, Ruschin M, Ma L, Verbakel W, Larson D, Brown PD. Stereotactic radiosurgery alone for multiple brain metastases? A review of clinical and technical issues. *Neuro Oncol.* 2017;19(suppl_2):ii2–ii15.
23. Ellingson BM, Bendszus M, Boxerman J, et al; Jumpstarting Brain Tumor Drug Development Coalition Imaging Standardization Steering Committee. Consensus recommendations for a standardized Brain Tumor Imaging Protocol in clinical trials. *Neuro Oncol.* 2015;17(9):1188–1198.
24. Lin NU, Lee EQ, Aoyama H, et al; Response Assessment in Neuro-Oncology (RANO) group. Response assessment criteria for brain metastases: proposal from the RANO group. *Lancet Oncol.* 2015;16(6):e270–e278.
25. Lin NU, Lee EQ, Aoyama H, et al; Response Assessment in Neuro-Oncology (RANO) group. Challenges relating to solid tumour brain metastases in clinical trials, part 1: patient population, response, and progression. A report from the RANO group. *Lancet Oncol.* 2013;14(10):e396–e406.
26. Lin NU, Wefel JS, Lee EQ, et al; Response Assessment in Neuro-Oncology (RANO) group. Challenges relating to solid tumour brain metastases in clinical trials, part 2: neurocognitive, neurological, and quality-of-life outcomes. A report from the RANO group. *Lancet Oncol.* 2013;14(10):e407–e416.
27. Mayr NA, Yuh WT, Muhonen MG, et al. Cost-effectiveness of high-dose MR contrast studies in the evaluation of brain metastases. *AJNR Am J Neuroradiol.* 1994;15(6):1053–1061.
28. Seute T, Leffers P, ten Velde GP, Twijnstra A. Detection of brain metastases from small cell lung cancer: consequences of changing imaging techniques (CT versus MRI). *Cancer.* 2008;112(8):1827–1834.
29. DiLuna ML, King JT Jr, Knisely JP, Chiang VL. Prognostic factors for survival after stereotactic radiosurgery vary with the number of cerebral metastases. *Cancer.* 2007;109(1):135–145.
30. Nussbaum ES, Djalilian HR, Cho KH, Hall WA. Brain metastases. Histology, multiplicity, surgery, and survival. *Cancer.* 1996;78(8):1781–1788.
31. Cagney DN, Martin AM, Catalano PJ, et al. Implications of screening for brain metastases in patients with breast cancer and non-small cell lung cancer. *JAMA Oncol.* 2018;4(7):1001–1003.
32. Delattre JY, Krol G, Thaler HT, Posner JB. Distribution of brain metastases. *Arch Neurol.* 1988;45(7):741–744.
33. Zhang M, Olsson Y. Hematogenous metastases of the human brain—characteristics of peritumoral brain changes: a review. *J Neurooncol.* 1997;35(1):81–89.
34. Lignelli A, Khandji AG. Review of imaging techniques in the diagnosis and management of brain metastases. *Neurosurg Clin N Am.* 2011;22(1):15–25, v.
35. Davis PC, Hudgins PA, Peterman SB, Hoffman JC Jr. Diagnosis of cerebral metastases: double-dose delayed CT vs contrast-enhanced MR imaging. *AJNR Am J Neuroradiol.* 1991;12(2):293–300.
36. Suzuki K, Yamamoto M, Hasegawa Y, et al. Magnetic resonance imaging and computed tomography in the diagnoses of brain metastases of lung cancer. *Lung Cancer.* 2004;46(3):357–360.
37. Schellinger PD, Meinck HM, Thron A. Diagnostic accuracy of MRI compared to CCT in patients with brain metastases. *J Neurooncol.* 1999;44(3):275–281.
38. Akeson P, Larsson EM, Kristoffersen DT, Jonsson E, Holtås S. Brain metastases—comparison of gadodiamide injection-enhanced MR imaging at standard and high dose, contrast-enhanced CT and non-contrast-enhanced MR imaging. *Acta Radiol.* 1995;36(3):300–306.
39. Soffietti R, Cornu P, Delattre JY, et al. EFNS guidelines on diagnosis and treatment of brain metastases: report of an EFNS Task Force. *Eur J Neurol.* 2006;13(7):674–681.
40. Soffietti R, Costanza A, Laguzzi E, Nobile M, Rudà R. Radiotherapy and chemotherapy of brain metastases. *J Neurooncol.* 2005;75(1):31–42.
41. Kaal EC, Niël CG, Vecht CJ. Therapeutic management of brain metastasis. *Lancet Neurol.* 2005;4(5):289–298.
42. Russell EJ, Geremia GK, Johnson CE, et al. Multiple cerebral metastases: detectability with Gd-DTPA-enhanced MR imaging. *Radiology.* 1987;165(3):609–617.
43. Healy ME, Hesselink JR, Press GA, Middleton MS. Increased detection of intracranial metastases with intravenous Gd-DTPA. *Radiology.* 1987;165(3):619–624.
44. Haustein J, Laniado M, Niendorf HP, et al. Administration of gadopentetate dimeglumine in MR imaging of intracranial tumors: dosage and field strength. *AJNR Am J Neuroradiol.* 1992;13(4):1199–1206.
45. Sze G, Milano E, Johnson C, Heier L. Detection of brain metastases: comparison of contrast-enhanced MR with unenhanced MR and enhanced CT. *AJNR Am J Neuroradiol.* 1990;11(4):785–791.
46. Kaal EC, Taphoorn MJ, Vecht CJ. Symptomatic management and imaging of brain metastases. *J Neurooncol.* 2005;75(1):15–20.
47. Egelhoff JC, Ross JS, Modic MT, Masaryk TJ, Estes M. MR imaging of metastatic GI adenocarcinoma in brain. *AJNR Am J Neuroradiol.* 1992;13(4):1221–1224.
48. Carrier DA, Mawad ME, Kirkpatrick JB, Schmid MF. Metastatic adenocarcinoma to the brain: MR with pathologic correlation. *AJNR Am J Neuroradiol.* 1994;15(1):155–159.
49. Oshiro S, Tsugu H, Komatsu F, et al. Metastatic adenocarcinoma in the brain: magnetic resonance imaging with pathological correlations to mucin content. *Anticancer Res.* 2008;28(1B):407–413.
50. Krabbe K, Gideon P, Wagn P, Hansen U, Thomsen C, Madsen F. MR diffusion imaging of human intracranial tumours. *Neuroradiology.* 1997;39(7):483–489.
51. Hayashida Y, Hirai T, Morishita S, et al. Diffusion-weighted imaging of metastatic brain tumors: comparison with histologic type and tumor cellularity. *AJNR Am J Neuroradiol.* 2006;27(7):1419–1425.
52. Goldman M, Boxerman JL, Rogg JM, Norén G. Utility of apparent diffusion coefficient in predicting the outcome of Gamma Knife–treated brain metastases prior to changes in tumor volume: a preliminary study. *J Neurosurg.* 2006;105 Suppl:175–182.
53. Mandybur TI. Intracranial hemorrhage caused by metastatic tumors. *Neurology.* 1977;27(7):650–655.
54. Franceschi AM, Moschos SJ, Anders CK, et al. Use of susceptibility-weighted imaging (SWI) in the detection of brain hemorrhagic metastases from breast cancer and melanoma. *J Comput Assist Tomogr.* 2016;40(5):803–805.
55. Downs RK, Bashir MH, Ng CK, Heidenreich JO. Quantitative contrast ratio comparison between T1 (TSE at 1.5T, FLAIR at 3T), magnetization prepared rapid gradient echo and subtraction imaging at 1.5T and 3T. *Quant Imaging Med Surg.* 2013;3(3):141–146.
56. Barkhof F, Pouwels PJ, Wattjes MP. The holy grail in diagnostic neuroradiology: 3T or 3D? *Eur Radiol.* 2011;21(3):449–456.
57. Soher BJ, Dale BM, Merkle EM. A review of MR physics: 3T versus 1.5T. *Magn Reson Imaging Clin N Am.* 2007;15(3):277–90, v.
58. Alvarez-Linera J. 3T MRI: advances in brain imaging. *Eur J Radiol.* 2008;67:415–426.
59. Nöbauer-Huhmann IM, Ba-Ssalamah A, Mlynarik V, et al. Magnetic resonance imaging contrast enhancement of brain tumors at 3 tesla versus 1.5 tesla. *Invest Radiol.* 2002;37(3):114–119.
60. Ba-Ssalamah A, Nöbauer-Huhmann IM, Pinker K, et al. Effect of contrast dose and field strength in the magnetic resonance detection of brain metastases. *Invest Radiol.* 2003;38(7):415–422.
61. Mugler JP 3rd. Optimized three-dimensional fast-spin-echo MRI. *J Magn Reson Imaging.* 2014;39(4):745–767.

62. Elster AD. How much contrast is enough? Dependence of enhancement on field strength and MR pulse sequence. *Eur Radiol.* 1997;7(Suppl 5):276–280.
63. Furutani K, Harada M, Mawlan M, Nishitani H. Difference in enhancement between spin echo and 3-dimensional fast spoiled gradient recalled acquisition in steady state magnetic resonance imaging of brain metastasis at 3-T magnetic resonance imaging. *J Comput Assist Tomogr.* 2008;32(2):313–319.
64. Kato Y, Higano S, Tamura H, et al. Usefulness of contrast-enhanced T1-weighted sampling perfection with application-optimized contrasts by using different flip angle evolutions in detection of small brain metastasis at 3T MR imaging: comparison with magnetization-prepared rapid acquisition of gradient echo imaging. *AJNR Am J Neuroradiol.* 2009;30(5):923–929.
65. Knauth M, Forsting M, Hartmann M, Heiland S, Balzer T, Sartor K. MR enhancement of brain lesions: increased contrast dose compared with magnetization transfer. *AJNR Am J Neuroradiol.* 1996;17(10):1853–1859.
66. Kakeda S, Korogi Y, Hiai Y, et al. Detection of brain metastasis at 3T: comparison among SE, IR-FSE and 3D-GRE sequences. *Eur Radiol.* 2007;17(9):2345–2351.
67. Takeda T, Takeda A, Nagaoka T, et al. Gadolinium-enhanced three-dimensional magnetization-prepared rapid gradient-echo (3D MP-RAGE) imaging is superior to spin-echo imaging in delineating brain metastases. *Acta Radiol.* 2008;49(10):1167–1173.
68. Suh CH, Jung SC, Kim KW, Pyo J. The detectability of brain metastases using contrast-enhanced spin-echo or gradient-echo images: a systematic review and meta-analysis. *J Neurooncol.* 2016;129(2):363–371.
69. Komada T, Naganawa S, Ogawa H, et al. Contrast-enhanced MR imaging of metastatic brain tumor at 3 tesla: utility of T(1)-weighted SPACE compared with 2D spin echo and 3D gradient echo sequence. *Magn Reson Med Sci.* 2008;7(1):13–21.
70. Nagao E, Yoshiura T, Hiwatashi A, et al. 3D turbo spin-echo sequence with motion-sensitized driven-equilibrium preparation for detection of brain metastases on 3T MR imaging. *AJNR Am J Neuroradiol.* 2011;32(4):664–670.
71. Park J, Kim J, Yoo E, Lee H, Chang JH, Kim EY. Detection of small metastatic brain tumors: comparison of 3D contrast-enhanced whole-brain black-blood imaging and MP-RAGE imaging. *Invest Radiol.* 2012;47(2):136–141.
72. Reichert M, Morelli JN, Runge VM, et al. Contrast-enhanced 3-dimensional SPACE versus MP-RAGE for the detection of brain metastases: considerations with a 32-channel head coil. *Invest Radiol.* 2013;48(1):55–60.
73. Chappell PM, Pelc NJ, Foo TK, Glover GH, Haros SP, Enzmann DR. Comparison of lesion enhancement on spin-echo and gradient-echo images. *AJNR Am J Neuroradiol.* 1994;15(1):37–44.
74. Majigsuren M, Abe T, Kageji T, et al. Comparison of brain tumor contrast-enhancement on T-1-CUBE and 3D-SPGR images. *Magn Reson Med Sci.* 2016;15(1):34–40.
75. Kammer NN, Coppenrath E, Treitl KM, Kooijman H, Dietrich O, Saam T. Comparison of contrast-enhanced modified T1-weighted 3D TSE black-blood and 3D MP-RAGE sequences for the detection of cerebral metastases and brain tumours. *Eur Radiol.* 2016;26(6):1818–1825.
76. Danieli L, Riccitelli GC, Distefano D, et al. Brain tumor-enhancement visualization and morphometric assessment: a comparison of MPRAGE, SPACE, and VIBE MRI techniques. *AJNR Am J Neuroradiol.* 2019;40(7):1140–1148.
77. Kim D, Heo YJ, Jeong HW, et al. Usefulness of the delay alternating with nutation for tailored excitation pulse with T1-weighted sampling perfection with application-optimized contrasts using different flip angle evolution in the detection of cerebral metastases: comparison with MPRAGE imaging. *AJNR Am J Neuroradiol.* 2019;40(9):1469–1475.
78. Samoudi AM, Van Audenhaege K, Vermeeren G, et al. Analysis of eddy currents induced by transverse and longitudinal gradient coils in different tungsten collimators geometries for SPECT/MRI integration. *Magn Reson Med.* 2015;74(6):1780–1789.
79. Bauknecht HC, Romano VC, Rogalla P, et al. Intra- and interobserver variability of linear and volumetric measurements of brain metastases using contrast-enhanced magnetic resonance imaging. *Invest Radiol.* 2010;45(1):49–56.
80. Hori M, Okubo T, Uozumi K, Ishigame K, Kumagai H, Araki T. T1-weighted fluid-attenuated inversion recovery at low field strength: a viable alternative for T1-weighted intracranial imaging. *AJNR Am J Neuroradiol.* 2003;24(4):648–651.
81. Al-Saeed O, Ismail M, Athyal RP, Rudwan M, Khafajee S. T1-weighted fluid-attenuated inversion recovery and T1-weighted fast spin-echo contrast-enhanced imaging: a comparison in 20 patients with brain lesions. *J Med Imaging Radiat Oncol.* 2009;53(4):366–372.
82. Shah KB, Guha-Thakurta N, Schellingerhout D, Madewell JE, Kumar AJ, Costelloe CM. Comparison of gadolinium-enhanced fat-saturated T1-weighted FLAIR and fast spin-echo MRI of the spine at 3 T for evaluation of extradural lesions. *AJR Am J Roentgenol.* 2011;197(3):697–703.
83. Vaneckova M, Herman M, Smith MP, et al. The benefits of high relaxivity for brain tumor imaging: results of a multicenter intraindividual crossover comparison of gadobenate dimeglumine with gadoterate meglumine (The BENEFIT Study). *AJNR Am J Neuroradiol.* 2015;36(9):1589–1598.
84. Anzalone N, Gerevini S, Scotti R, Vezzulli P, Picozzi P. Detection of cerebral metastases on magnetic resonance imaging: intraindividual comparison of gadobutrol with gadopentetate dimeglumine. *Acta Radiol.* 2009;50(8):933–940.
85. Anzalone N, Scarabino T, Venturi C, et al. Cerebral neoplastic enhancing lesions: multicenter, randomized, crossover intraindividual comparison between gadobutrol (1.0M) and gadoterate meglumine (0.5M) at 0.1 mmol Gd/kg body weight in a clinical setting. *Eur J Radiol.* 2013;82(1):139–145.
86. Kim ES, Chang JH, Choi HS, Kim J, Lee SK. Diagnostic yield of double-dose gadobutrol in the detection of brain metastasis: intraindividual comparison with double-dose gadopentetate dimeglumine. *AJNR Am J Neuroradiol.* 2010;31(6):1055–1058.
87. Katakami N, Inaba Y, Sugata S, et al. Magnetic resonance evaluation of brain metastases from systemic malignances with two doses of gadobutrol 1.0 m compared with gadoteridol: a multicenter, phase ii/iii study in patients with known or suspected brain metastases. *Invest Radiol.* 2011;46(7):411–418.
88. Sze G, Johnson C, Kawamura Y, et al. Comparison of single- and triple-dose contrast material in the MR screening of brain metastases. *AJNR Am J Neuroradiol.* 1998;19(5):821–828.
89. Yuh WT, Tali ET, Nguyen HD, Simonson TM, Mayr NA, Fisher DJ. The effect of contrast dose, imaging time, and lesion size in the MR detection of intracerebral metastasis. *AJNR Am J Neuroradiol.* 1995;16(2):373–380.
90. Yuh WT, Engelken JD, Muhonen MG, Mayr NA, Fisher DJ, Ehrhardt JC. Experience with high-dose gadolinium MR imaging in the evaluation of brain metastases. *AJNR Am J Neuroradiol.* 1992;13(1):335–345.
91. Subedi KS, Takahashi T, Yamano T, et al. Usefulness of double dose contrast-enhanced magnetic resonance imaging for clear delineation of gross tumor volume in stereotactic radiotherapy treatment planning of metastatic brain tumors: a dose comparison study. *J Radiat Res.* 2013;54(1):135–139.
92. Haustein J, Laniado M, Niendorf HP, et al. Triple-dose versus standard-dose gadopentetate dimeglumine: a randomized study in 199 patients. *Radiology.* 1993;186(3):855–860.

93. Runge VM, Kirsch JE, Burke VJ, et al. High-dose gadoteridol in MR imaging of intracranial neoplasms. *J Magn Reson Imaging.* 1992;2(1):9–18.
94. Runge VM, Kirsch JE, Thomas GS. High-dose applications of gadolinium chelates in magnetic resonance imaging. *Magn Reson Med.* 1991;22(2):358–363.
95. Schubeus P, Schorner W, Haustein J. Dosing of Gd-DTPA in MR imaging of intracranial tumors. *Magn Reson Med.* 1991;22(2):249–254; discussion 265–267.
96. Van Dijk P, Sijens PE, Schmitz PI, Oudkerk M. Gd-enhanced MR imaging of brain metastases: contrast as a function of dose and lesion size. *Magn Reson Imaging.* 1997;15(5):535–541.
97. Yuh WT, Fisher DJ, Runge VM, et al. Phase III multicenter trial of high-dose gadoteridol in MR evaluation of brain metastases. *AJNR Am J Neuroradiol.* 1994;15(6):1037–1051.
98. Kushnirsky M, Nguyen V, Katz JS, et al. Time-delayed contrast-enhanced MRI improves detection of brain metastases and apparent treatment volumes. *J Neurosurg.* 2016;124(2):489–495.
99. Cohen-Inbar O, Xu Z, Dodson B, et al. Time-delayed contrast-enhanced MRI improves detection of brain metastases: a prospective validation of diagnostic yield. *J Neurooncol.* 2016;130(3):485–494.
100. McDonald RJ, McDonald JS, Kallmes DF, et al. Intracranial gadolinium deposition after contrast-enhanced MR imaging. *Radiology.* 2015;275(3):772–782.
101. Kaewlai R, Abujudeh H. Nephrogenic systemic fibrosis. *AJR Am J Roentgenol.* 2012;199(1):W17–W23.
102. Jeon JY, Choi JW, Roh HG, Moon WJ. Effect of imaging time in the magnetic resonance detection of intracerebral metastases using single dose gadobutrol. *Korean J Radiol.* 2014;15(1):145–150.
103. Yoon BC, Saad AF, Rezaii P, Wintermark M, Zaharchuk G, Iv M. Evaluation of thick-slab overlapping mip images of contrast-enhanced 3D T1-weighted CUBE for detection of intracranial metastases: a pilot study for comparison of lesion detection, interpretation time, and sensitivity with nonoverlapping CUBE MIP, CUBE, and inversion-recovery-prepared fast-spoiled gradient recalled brain volume. *AJNR Am J Neuroradiol.* 2018;39(9):1635–1642.
104. Fukuoka H, Hirai T, Okuda T, et al. Comparison of the added value of contrast-enhanced 3D fluid-attenuated inversion recovery and magnetization-prepared rapid acquisition of gradient echo sequences in relation to conventional postcontrast T1-weighted images for the evaluation of leptomeningeal diseases at 3T. *AJNR Am J Neuroradiol.* 2010;31(5):868–873.
105. Oh J, Choi SH, Lee E, et al. Application of 3D fast spin-echo T1 black-blood imaging in the diagnosis and prognostic prediction of patients with leptomeningeal carcinomatosis. *AJNR Am J Neuroradiol.* 2018;39(8):1453–1459.
106. Chamberlain M, Junck L, Brandsma D, et al. Leptomeningeal metastases: a RANO proposal for response criteria. *Neuro Oncol.* 2017;19(4):484–492.
107. Le Rhun E, Devos P, Boulanger T, et al. The RANO Leptomeningeal Metastasis Group proposal to assess response to treatment: lack of feasibility and clinical utility, and a revised proposal. *Neuro Oncol.* 2019;21(5):648–658.
108. Narloch JL, Farber SH, Sammons S, et al. Biopsy of enlarging lesions after stereotactic radiosurgery for brain metastases frequently reveals radiation necrosis. *Neuro Oncol.* 2017;19(10):1391–1397.
109. Nath SK, Sheridan AD, Rauch PJ, et al. Significance of histology in determining management of lesions regrowing after radiosurgery. *J Neurooncol.* 2014;117(2):303–310.
110. Patel TR, McHugh BJ, Bi WL, Minja FJ, Knisely JP, Chiang VL. A comprehensive review of MR imaging changes following radiosurgery to 500 brain metastases. *AJNR Am J Neuroradiol.* 2011;32(10):1885–1892.
111. Kohutek ZA, Yamada Y, Chan TA, et al. Long-term risk of radionecrosis and imaging changes after stereotactic radiosurgery for brain metastases. *J Neurooncol.* 2015;125(1):149–156.
112. Colaco RJ, Martin P, Kluger HM, Yu JB, Chiang VL. Does immunotherapy increase the rate of radiation necrosis after radiosurgical treatment of brain metastases? *J Neurosurg.* 2016;125(1):17–23.
113. Dequesada IM, Quisling RG, Yachnis A, Friedman WA. Can standard magnetic resonance imaging reliably distinguish recurrent tumor from radiation necrosis after radiosurgery for brain metastases? A radiographic-pathological study. *Neurosurgery.* 2008;63(5):898–903; discussion 904.
114. Stockham AL, Tievsky AL, Koyfman SA, et al. Conventional MRI does not reliably distinguish radiation necrosis from tumor recurrence after stereotactic radiosurgery. *J Neurooncol.* 2012;109(1):149–158.
115. Leeman JE, Clump DA, Flickinger JC, Mintz AH, Burton SA, Heron DE. Extent of perilesional edema differentiates radionecrosis from tumor recurrence following stereotactic radiosurgery for brain metastases. *Neuro Oncol.* 2013;15(12):1732–1738.
116. Wagner S, Lanfermann H, Eichner G, Gufler H. Radiation injury versus malignancy after stereotactic radiosurgery for brain metastases: impact of time-dependent changes in lesion morphology on MRI. *Neuro Oncol.* 2017;19(4):586–594.
117. Lee CC, Wintermark M, Xu Z, Yen CP, Schlesinger D, Sheehan JP. Application of diffusion-weighted magnetic resonance imaging to predict the intracranial metastatic tumor response to gamma knife radiosurgery. *J Neurooncol.* 2014;118(2):351–361.
118. Jakubovic R, Zhou S, Heyn C, et al. The predictive capacity of apparent diffusion coefficient (ADC) in response assessment of brain metastases following radiation. *Clin Exp Metastasis.* 2016;33(3):277–284.
119. Knitter JR, Erly WK, Stea BD, et al. Interval change in diffusion and perfusion MRI parameters for the assessment of pseudoprogression in cerebral metastases treated with stereotactic radiation. *AJR Am J Roentgenol.* 2018;211(1):168–175.
120. Chernov MF, Ono Y, Abe K, et al. Differentiation of tumor progression and radiation-induced effects after intracranial radiosurgery. *Acta Neurochir Suppl.* 2013;116:193–210.
121. Nakajima T, Kumabe T, Kanamori M, et al. Differential diagnosis between radiation necrosis and glioma progression using sequential proton magnetic resonance spectroscopy and methionine positron emission tomography. *Neurol Med Chir (Tokyo).* 2009;49(9):394–401.
122. Lai G, Mahadevan A, Hackney D, et al. Diagnostic accuracy of PET, SPECT, and arterial spin-labeling in differentiating tumor recurrence from necrosis in cerebral metastasis after stereotactic radiosurgery. *AJNR Am J Neuroradiol.* 2015;36(12):2250–2255.
123. Almeida-Freitas DB, Pinho MC, Otaduy MC, Braga HF, Meira-Freitas D, da Costa Leite C. Assessment of irradiated brain metastases using dynamic contrast-enhanced magnetic resonance imaging. *Neuroradiology.* 2014;56(6):437–443.
124. Koh MJ, Kim HS, Choi CG, Kim SJ. Which is the best advanced MR imaging protocol for predicting recurrent metastatic brain tumor following gamma-knife radiosurgery: focused on perfusion method. *Neuroradiology.* 2015;57(4):367–376.
125. Taunk NK, Oh JH, Shukla-Dave A, et al. Early posttreatment assessment of MRI perfusion biomarkers can predict long-term response of lung cancer brain metastases to stereotactic radiosurgery. *Neuro Oncol.* 2018;20(4):567–575.
126. Barajas RF, Chang JS, Sneed PK, Segal MR, McDermott MW, Cha S. Distinguishing recurrent intra-axial metastatic tumor from radiation necrosis following gamma knife radiosurgery using dynamic susceptibility-weighted contrast-enhanced perfusion MR imaging. *AJNR Am J Neuroradiol.* 2009;30(2):367–372.

127. Hoefnagels FW, Lagerwaard FJ, Sanchez E, et al. Radiological progression of cerebral metastases after radiosurgery: assessment of perfusion MRI for differentiating between necrosis and recurrence. *J Neurol*. 2009;256(6):878–887.
128. Mitsuya K, Nakasu Y, Horiguchi S, et al. Perfusion weighted magnetic resonance imaging to distinguish the recurrence of metastatic brain tumors from radiation necrosis after stereotactic radiosurgery. *J Neurooncol*. 2010;99(1):81–88.
129. Kimura T, Sako K, Tanaka K, et al. Evaluation of the response of metastatic brain tumors to stereotactic radiosurgery by proton magnetic resonance spectroscopy, 201TICI single-photon emission computerized tomography, and gadolinium-enhanced magnetic resonance imaging. *J Neurosurg*. 2004;100(5):835–841.
130. Tomura N, Kokubun M, Saginoya T, Mizuno Y, Kikuchi Y. Differentiation between treatment-induced necrosis and recurrent tumors in patients with metastatic brain tumors: comparison among 11C-methionine-PET, FDG-PET, MR permeability imaging, and MRI-ADC-preliminary results. *AJNR Am J Neuroradiol*. 2017;38(8):1520–1527.
131. Ceccon G, Lohmann P, Stoffels G, et al. Dynamic O-(2-18F-fluoroethyl)-L-tyrosine positron emission tomography differentiates brain metastasis recurrence from radiation injury after radiotherapy. *Neuro Oncol*. 2017;19(2):281–288.
132. Galldiks N, Stoffels G, Filss CP, et al. Role of O-(2-(18)F-fluoroethyl)-L-tyrosine PET for differentiation of local recurrent brain metastasis from radiation necrosis. *J Nucl Med*. 2012;53(9):1367–1374.
133. Lizarraga KJ, Allen-Auerbach M, Czernin J, et al. (18)F-FDOPA PET for differentiating recurrent or progressive brain metastatic tumors from late or delayed radiation injury after radiation treatment. *J Nucl Med*. 2014;55(1):30–36.
134. Lohmann P, Kocher M, Ceccon G, et al. Combined FET PET/MRI radiomics differentiates radiation injury from recurrent brain metastasis. *Neuroimage Clin*. 2018;20:537–542.
135. Li H, Deng L, Bai HX, et al. Diagnostic accuracy of amino acid and FDG-PET in differentiating brain metastasis recurrence from radionecrosis after radiotherapy: a systematic review and meta-analysis. *AJNR Am J Neuroradiol*. 2018;39(2):280–288.
136. Leiva-Salinas C, Muttikkal TJE, Flors L, et al. FDG PET/MRI coregistration helps predict response to gamma knife radiosurgery in patients with brain metastases. *AJR Am J Roentgenol*. 2019;212(2):425–430.
137. Suh CH, Kim HS, Jung SC, Choi CG, Kim SJ. Comparison of MRI and PET as potential surrogate endpoints for treatment response after stereotactic radiosurgery in patients with brain metastasis. *AJR Am J Roentgenol*. 2018;211(6):1332–1341.
138. Grkovski M, Kohutek ZA, Schoder H, et al. (18)F-fluorocholine PET uptake correlates with pathologic evidence of recurrent tumor after stereotactic radiosurgery for brain metastases. *Eur J Nucl Med Mol Imaging*. 2019. doi:10.1007/s00259-019-04628-6.
139. Pope WB. Brain metastases: neuroimaging. *Handb Clin Neurol*. 2018;149:89–112.
140. Galldiks N, Langen KJ, Albert NL, et al. PET imaging in patients with brain metastasis-report of the RANO/PET group. *Neuro Oncol*. 2019;21(5):585–595.
141. Zach L, Guez D, Last D, et al. Delayed contrast extravasation MRI: a new paradigm in neuro-oncology. *Neuro Oncol*. 2015;17(3):457–465.
142. Zach L, Guez D, Last D, et al. Delayed contrast extravasation MRI for depicting tumor and non-tumoral tissues in primary and metastatic brain tumors. *PLoS One*. 2012;7(12):e52008.
143. Wang B, Zhang Y, Zhao B, et al. Postcontrast T1 mapping for differential diagnosis of recurrence and radionecrosis after gamma knife radiosurgery for brain metastasis. *AJNR Am J Neuroradiol*. 2018;39(6):1025–1031.
144. Prasanna P, Rogers L, Lam TC, et al. Disorder in pixel-level edge directions on T1WI Is associated with the degree of radiation necrosis in primary and metastatic brain tumors: preliminary findings. *AJNR Am J Neuroradiol*. 2019;40(3):412–417.
145. Peng L, Parekh V, Huang P, et al. Distinguishing true progression from radionecrosis after stereotactic radiation therapy for brain metastases with machine learning and radiomics. *Int J Radiat Oncol Biol Phys*. 2018;102(4):1236–1243.
146. Schmainda KM, Prah MA, Hu LS, et al. Moving toward a consensus DSC-MRI protocol: validation of a low-flip angle single-dose option as a reference standard for brain tumors. *AJNR Am J Neuroradiol*. 2019;40(4):626–633.
147. Semmineh NB, Bell LC, Stokes AM, Hu LS, Boxerman JL, Quarles CC. Optimization of acquisition and analysis methods for clinical dynamic susceptibility contrast MRI using a population-based digital reference object. *AJNR Am J Neuroradiol*. 2018;39(11):1981–1988.
148. Leu K, Boxerman JL, Ellingson BM. Effects of MRI protocol parameters, preload injection dose, fractionation strategies, and leakage correction algorithms on the fidelity of dynamic-susceptibility contrast MRI estimates of relative cerebral blood volume in gliomas. *AJNR Am J Neuroradiol*. 2017;38(3):478–484.
149. Willats L, Calamante F. The 39 steps: evading error and deciphering the secrets for accurate dynamic susceptibility contrast MRI. *NMR Biomed*. 2013;26(8):913–931.
150. Okada H, Weller M, Huang R, et al. Immunotherapy Response Assessment in Neuro-Oncology: a report of the RANO working group. *Lancet Oncol*. 2015;16(15):e534–e542.
151. Kebir S, Rauschenbach L, Galldiks N, et al. Dynamic O-(2-[18F]fluoroethyl)-L-tyrosine PET imaging for the detection of checkpoint inhibitor-related pseudoprogression in melanoma brain metastases. *Neuro Oncol*. 2016;18(10):1462–1464.
152. Yamada K, Kubota H, Kizu O, et al. Effect of intravenous gadolinium-DTPA on diffusion-weighted images: evaluation of normal brain and infarcts. *Stroke*. 2002;33(7):1799–1802.